Unlimited Sampling via One-Bit Quantization

Arian Eamaz†, Kumar Vijay Mishra‡, Farhang Yeganegi†, and Mojtaba Soltanalian†
†University of Illinois, Chicago, IL 60607, USA
‡United States DEVCOM Army Research Laboratory, Adelphi, MD 20783 USA

***Abstract*—Shannon's sampling theorem plays a central role in the discrete-time processing of bandlimited signals. However, the infinite precision assumed by Shannon's theorem is impractical because of the ADC clipping effect that limits the signal's dynamic range. Moreover, the power consumption of an analog-to-digital converter (ADC) increases linearly with the sampling frequency and may be prohibitively high for a wide bandwidth signal. Recently, unlimited and one-bit sampling frameworks have been proposed to address these shortcomings. The former is a high-resolution technique that employs *self-reset ADCs* to achieve an unlimited dynamic range. The latter achieves relatively low cost and reduced power consumption at an elevated sampling rate. In this paper, we examine jointly exploiting the appealing attributes of both techniques. We propose *un*limited *o*ne-bit (UNO) sampling, which entails a judicious design of one-bit sampling thresholds. This enables storing the distance between the input signal value and the threshold. We then utilize this information to accurately reconstruct the signal from its one-bit samples via a *randomized Kaczmarz algorithm* (RKA) which is considered to be a strong linear feasibility solver that selects a random linear equation in each iteration. The numerical results illustrate the effectiveness of RKA-based UNO over the state-of-the-art.**

***Index Terms*—One-bit quantization, unlimited sampling, self-reset ADCs, signal reconstruction, time-varying sampling thresholds.**

I. Introduction

Sampling theory lies at the heart of all modern digital signal processing systems. A seminal result in the sampling literature is the Whittaker-Kotelńikov-Shannon (or, simply Shannon's) theorem, which states that a lowpass bandlimited signal can be perfectly reconstructed from its discrete samples taken uniformly at a sampling frequency that is at least the Nyquist rate, i.e., twice the signal bandwidth [1–3]. However, practical implementations of this result are beset with hardware limitations. For example, the theorem operates under an impractical assumption of the availability of infinite precision samples. In practice, digital sampling is realized by quantizing the signals-of-interest through analog-to-digital converters (ADCs) that clip or saturate whenever the signal amplitude exceeds the maximum recordable ADC voltage, leading to a significant information loss. Substantial work has been done and is still ongoing to overcome this problem [4–7], and the approaches are too diverse to summarize here; see, e.g., [8] and references therein, for comparisons of various techniques. Overall, these approaches require de-clipping [9], multiple ADCs [10], and scaling techniques [11], which are expensive and cumbersome. On the other hand, the recently proposed *unlimited sampling* framework fully overcomes this limitation by employing modular arithmetic [8, 12, 13].

Note that conventional ADCs require a large number of bits to sample the original continuous signal with low quantization errors. Sampling at high rates with high-resolution ADCs, however, dramatically increases the power consumption and the manufacturing cost [14]. This problem is exacerbated in systems that require multiple ADCs such as large array receivers [15]. Therefore, in recent years, the design of receivers with low-complexity *one-bit ADC* has been emphasized to meet the requirements of both wide signal bandwidth and low cost/power. The *one-bit quantization* is an extreme scenario, wherein the ADCs merely compare the signals with given or known threshold levels, producing one-bit sign (± 1) outputs [16, 17], thereby considerably bringing down the analog complexity of the receiver. The classical clipping-based sampling [18, 19] also yields one-bit samples but the signal recovery is achieved by comparing the signal with a zero threshold. In lieu of signal reconstruction, the objective of these techniques is to recover the signal's autocorrelation, yet the clipped output is not guaranteed to yield accurate estimates. In this context, recent investigations using time-varying sampling thresholds have shown better estimation performance [20–22].

Evidently, one-bit and unlimited sampling frameworks address complementary requirements. One-bit sampling is indifferent to the dynamic range because, apart from the comparison bit, other information such as the distance between the signal value and the threshold is not stored. On the other hand, the self-reset ADC in unlimited sampling provides a natural approach to producing judicious time-varying thresholds for one-bit ADCs. In this paper, to harness the advantages of both methods, we propose *un*limited *o*ne-bit (UNO) sampling that yields unlimited dynamic range and a low-cost low-power receiver while retaining a high sampling rate. There is a related body of literature on consistent reconstruction methods for oversampled frames from sparse samples [23] and one-bit quantized measurements [24–26]. However, these studies differ from UNO in two key aspects. Firstly, they did not incorporate the practice of unlimited sampling at the core of their sampling methodology, which involves folding the signal within the range of the ADC threshold. Secondly, these earlier works assign multiple bits to each measurement value using a multi-bit quantizer. On the contrary, we compare modulo samples with multiple time-varying threshold sequences. This approach has the benefits of one-bit measurements, including robustness to certain nonlinearities (e.g., ADC saturation) in signal acquisition. The reconstructing of the input signal is more challenging in UNO because its quantizer provides only low-resolution (one-bit) data.

Among prior studies, state-of-the-art results in [27] proposed *one-bit $\Sigma\Delta$ quantization via unlimited sampling*, whose objective is to shrink the *dynamic range between the input signal and its one-bit samples*. This study developed a guaranteed reconstruction as long as the dynamic range of the input signal is less than the dynamic range of the one-bit data (i.e., 1). However, when the ratio of the input signal amplitude to the ADC threshold is large, then the imperfect noise shaping in sigma-delta conversion degrades this reconstruction. Contrary to this approach, our proposed UNO technique focuses on a different problem, i.e., shrinking the *dynamic range between the input signal and the time-varying sampling thresholds*. The UNO framework offers arbitrary time-varying sampling thresholds; thus, effectively reducing the gap between the input signal and the time-varying sampling thresholds. To reconstruct the full-precision signal

Corresponding author: A. Eamaz (e-mail: aeamaz2@uic.edu).
This work was supported in part by the National Science Foundation Grant CCF-1704401.

from one-bit sampled data, conventional approaches include maximum likelihood estimation (MLE) and weighted least squares [28]. However, these methods have high computational cost, especially for high-dimensional input signals. To this end, we propose using the randomized Kaczmarz algorithm (RKA) [29, 30], which is an iterative algorithm for solving a system of linear equations. The RKA is simple to implement and performs comparably with the state-of-the-art optimization methods. While the deterministic version of the Kaczmarz method usually selects the linear equation sequentially, the RKA is randomized in its selection at each iteration which can lead to a faster convergence.

Throughout this paper, we use boldface lowercase, boldface uppercase, and calligraphic letters for vectors, matrices, and sets, respectively. The notations $\mathbb{C}$, $\mathbb{R}$, and $\mathbb{Z}$ represent the set of complex, real, and integer numbers, respectively. We represent a vector $\mathbf{x}$ in terms of its elements $\{x_i\}$ as $\mathbf{x} = [x_i]$. We use $(\cdot)^\top$ and $(\cdot)^{\mathrm{H}}$ to denote the vector/matrix transpose, and the Hermitian transpose, respectively. We define $\mathbf{x} \succeq \mathbf{y}$ as a component-wise inequality between vectors $\mathbf{x}$ and $\mathbf{y}$, i.e., $x_i \geq y_i$ for every index i [31, p. 32]. The max-norm ($p \to \infty$) of a function x is defined as, $\|x\|_\infty = \inf\{c_0 \geq 0 : |x(t)| \leq c_0\}$, where $\inf(\cdot)$ denotes the infimum of its argument; for vectors, we have $\|\mathbf{x}\|_\infty = \max_k |x_k|$. The Frobenius norm is denoted by $\|\cdot\|_{\mathrm{F}}$. The function $\mathrm{diag}(\cdot)$ outputs a diagonal matrix with the input vector along its main diagonal. For a vector $\mathbf{x}$, $\Delta\mathbf{x} = x_{k+1} - x_k$ denotes the finite difference and recursively applying the same yields N-th order difference, $\Delta^N\mathbf{x}$. We denote the Ω-bandlimited Paley-Wiener subspace of the square-integrable function space L^2 by PW_Ω. The Hadamard (element-wise) product of two matrices $\mathbf{B}_1$ and $\mathbf{B}_2$ is denoted as $\mathbf{B}_1 \odot \mathbf{B}_2$. The vectorized form of a matrix $\mathbf{B}$ is written as $\mathrm{vec}(\mathbf{B})$. Given a scalar x, we define the operator $(x)^+$ as $\max\{x, 0\}$. For an event $\mathcal{E}$, $\mathbb{1}_{(\mathcal{E})}$ is the indicator function for that event meaning that $\mathbb{1}_{(\mathcal{E})}$ is 1 if $\mathcal{E}$ occurs; otherwise, it is zero. The function $\mathrm{sgn}(\cdot)$ yields the sign of its argument. The floor operation is denoted by $\lfloor\rfloor$.

II. One-Bit Sampling

Consider a bandlimited continuous-time signal $x \in \mathrm{PW}_\Omega$ that we represent via Shannon's sampling theorem as [3]

$$x(t) = \sum_{k=-\infty}^{k=+\infty} x(k\mathrm{T})\,\mathrm{sinc}\left(\frac{t}{\mathrm{T}} - k\right), \quad 0 < \mathrm{T} \leqslant \frac{\pi}{\Omega}, \tag{1}$$

where $1/\mathrm{T}$ is the sampling rate, Ω is the signal bandwidth, and $\mathrm{sinc}(t) = \frac{\sin(\pi t)}{\pi t}$ is an *ideal* low-pass filter. Denote the uniform samples of $x(t)$ with the sampling rate $1/\mathrm{T}$ by $x_k = x(k\mathrm{T})$.

In practice, the discrete-time samples occupy pre-determined quantized values. We denote the quantization operation on x_k by the function $Q(\cdot)$. This yields the quantized signal as

$$r_k = Q(x_k). \tag{2}$$

In one-bit quantization, compared to zero or constant thresholds, time-varying sampling thresholds yield a better recovery performance [14, 22]. These thresholds may be chosen from any distribution. In this work, to be consistent with the state-of-the-art [14, 19, 28], we consider a Gaussian non-zero time-varying threshold vector $\boldsymbol{\tau}_{\mathcal{N}} = [\tau_k]$ that follows the distribution $\boldsymbol{\tau}_{\mathcal{N}} \sim \mathcal{N}(\mathbf{d} = \mathbf{1}d, \boldsymbol{\Sigma})$. Following a bell-shaped distribution, a Gaussian threshold is likely to be concentrated in the center and may not cover the entire signal range accurately. Therefore, alternatively, we also employ uniformly distributed thresholds in the sequel as $\boldsymbol{\tau}_{\mathcal{U}} \sim \mathcal{U}_{[a,b]}$. In the case of one-bit quantization with such time-varying sampling thresholds, $r_k = \mathrm{sgn}(x_k - \tau_k)$. For notational simplicity, hereafter, we denote the time-varying sampling thresholds by dropping the subscripts, i.e. $\boldsymbol{\tau} = [\tau_k]$.

The information gathered through the one-bit sampling with time-varying thresholds may be formulated in terms of an overdetermined linear system of inequalities. We have $r_k = +1$ when $x_k > \tau_k$ and $r_k = -1$ when $x_k < \tau_k$. Therefore, one can formulate the geometric location of the signal as $r_k(x_k - \tau_k) \geq 0$. Collecting all the elements in the vectors as $\mathbf{x} = [x_k] \in \mathbb{R}^n$ and $\mathbf{r} = [r_k] \in \mathbb{R}^n$, we have

$$\mathbf{r} \odot (\mathbf{x} - \boldsymbol{\tau}) \succeq \mathbf{0}, \tag{3}$$

or equivalently

$$\boldsymbol{\Omega}\mathbf{x} \succeq \mathbf{r} \odot \boldsymbol{\tau}, \tag{4}$$

where $\boldsymbol{\Omega} \triangleq \mathrm{diag}(\mathbf{r})$. Denote the time-varying sampling threshold in ℓ-th signal sequence by $\boldsymbol{\tau}^{(\ell)}$, where $\ell \in \mathcal{L} = \{1, \cdots, m\}$. It follows from (4) that

$$\boldsymbol{\Omega}^{(\ell)}\mathbf{x} \succeq \mathbf{r}^{(\ell)} \odot \boldsymbol{\tau}^{(\ell)}, \quad \ell \in \mathcal{L}, \tag{5}$$

where the sign matrix $\boldsymbol{\Omega}^{(\ell)} = \mathrm{diag}\left(\mathbf{r}^{(\ell)}\right)$. Denote the concatenation of all m sign matrices as

$$\tilde{\boldsymbol{\Omega}} = \left[\ \boldsymbol{\Omega}^{(1)} \ \middle|\ \cdots \ \middle|\ \boldsymbol{\Omega}^{(m)}\ \right]^\top, \quad \tilde{\boldsymbol{\Omega}} \in \mathbb{R}^{mn \times n}. \tag{6}$$

Rewrite the m linear inequalities in (5) as

$$\tilde{\boldsymbol{\Omega}}\mathbf{x} \succeq \mathrm{vec}(\mathbf{R}) \odot \mathrm{vec}(\boldsymbol{\Gamma}), \tag{7}$$

where $\mathbf{R}$ and $\boldsymbol{\Gamma}$ are matrices, whose columns are the sequences $\left\{\mathbf{r}^{(\ell)}\right\}_{\ell=1}^m$ and $\left\{\boldsymbol{\tau}^{(\ell)}\right\}_{\ell=1}^m$, respectively.

The linear system of inequalities in (7) associated with the one-bit sampling scheme is overdetermined. We recast (7) into a *one-bit polyhedron* as

$$\mathcal{P} = \left\{\mathbf{x} \mid \tilde{\boldsymbol{\Omega}}\mathbf{x} \succeq \mathrm{vec}(\mathbf{R}) \odot \mathrm{vec}(\boldsymbol{\Gamma})\right\}. \tag{8}$$

Instead of complex high-dimensional optimization with techniques such as MLE, our objective is to employ the polyhedron (8) that encapsulates the desired signal $\mathbf{x}$, which leads to solving a system of linear inequalities with linear convergence in expectation.

III. Unlimited Sampling

In unlimited sampling, instead of point-wise samples of the bandlimited function $x(t)$, the *folded amplitudes* with values in the range $[-\lambda, \lambda]$, where $\lambda > 0$ is the ADC threshold, are used [8, 12]. The folding corresponds to introducing a non-linearity in the sensing process [8, 12] and is denoted by the modulo operator $\mathcal{M}_\lambda$ as

$$\mathcal{M}_\lambda : \quad \tilde{x}_k = x_k - 2\lambda\left\lfloor\frac{x_k}{2\lambda} + \frac{1}{2}\right\rfloor, \tag{9}$$

where $\tilde{x}_k$ are the modulo samples of $x(t)$, respectively. According to the unlimited sampling theorem [8], the required condition for the perfect reconstruction of the input signal from its modulo samples, is $T \leq \frac{1}{2\Omega_{\max} e}$, where $\Omega_{\max}$ denotes the maximum frequency of the input bandlimited signal and e is the Euler's number.

The following process is a stepping stone towards the reconstruction of the bandlimited function $x(t)$ from its modulo samples $\{\tilde{x}_k\}$. Then, $x(t)$ admits a decomposition [8, 12],

$$x(t) = \tilde{x}(t) + \epsilon_x(t), \tag{10}$$

where $\tilde{x}(t) = \mathcal{M}_\lambda(x(t))$ and the error ϵ_x between the input signal and its modulo samples is

$$\epsilon_x(t) = 2\lambda\sum_{u\in\mathbb{Z}} e_u \mathbb{1}_{\mathcal{D}_u}(t), \quad e_u \in \mathbb{Z}, \tag{11}$$

where $\bigcup_{u\in\mathbb{Z}} \mathcal{D}_u = \mathbb{R}$ is a partition of the real line into intervals $\mathcal{D}_u$.

It follows from (11) that ϵ_x takes only those values that are integer multiples of 2λ thereby leading to a robust reconstruction algorithm [8]. Specifically, to obtain ϵ_x (up to an unknown additive constant)

and subsequently the desired signal $x(t)$, the reconstruction procedure in [8, 12] requires the higher-order differences of $\tilde{\mathbf{x}} = [\tilde{x}_k]$ to obtain $\Delta^N \boldsymbol{\epsilon}_x = \mathcal{M}_\lambda\left(\Delta^N \tilde{\mathbf{x}}\right) - \Delta^N \tilde{\mathbf{x}}$, where $\boldsymbol{\epsilon}_x = [\epsilon_x]$. Define the inverse-difference operator as a sum of real sequence $\{s_b\}$, i.e.,

$$\nabla : \{s_k\}_{k\in\mathbb{Z}^+} \rightarrow \sum_{b=1}^{k} s_b. \tag{12}$$

Then, applying $\nabla\left(\Delta^N \boldsymbol{\epsilon}_x\right)$ and rounding the result to the nearest multiple of $2\lambda\mathbb{Z}$ yields ϵ_x. For a guaranteed and stable reconstruction performance, a suitable choice for difference order N is [8],

$$N \geq \left\lceil \frac{\log\lambda - \log\beta_x}{\log\left(T\Omega e\right)} \right\rceil, \tag{13}$$

where β_x is chosen such that $\beta_x \in 2\lambda\mathbb{Z}$ and $\|x\|_\infty \leq \beta_x$.

IV. Proposed UNO Framework

The dynamic range of a signal $\mathbf{x}$ is defined as $\mathrm{DR}_{\mathbf{x}} = \|\mathbf{x}\|_\infty$. Denote the dynamic ranges of the desired signal $\mathbf{x}$ and the time-varying threshold $\boldsymbol{\tau}$ by $\mathrm{DR}_{\mathbf{x}}$ and $\mathrm{DR}_{\boldsymbol{\tau}}$, respectively. If $\mathrm{DR}_{\mathbf{x}} \leq \mathrm{DR}_{\boldsymbol{\tau}}$, then the reconstructed signal $\mathbf{x}^\star$ may be found inside the polyhedron (8) with a high probability for an *adequate* number of samples. Otherwise, if $\mathrm{DR}_{\mathbf{x}} > \mathrm{DR}_{\boldsymbol{\tau}}$, there is no guarantee to obtain $\mathbf{x}^\star$ since the desired solution cannot be inside the finite-volume space imposed by the set of inequalities in (8) indicating an irretrievable information loss. We demonstrate this as follows. Without loss of generality, consider $x_k > 0$. Assume $x_k = \mathrm{DR}_{\mathbf{x}}$ and the maximum threshold $\tau_k^\star = \max_\ell \tau_k^{(\ell)}$. Since $\mathrm{DR}_{\boldsymbol{\tau}} = \|\boldsymbol{\tau}\|_\infty$, we have $\tau_k^\star \leq \mathrm{DR}_{\boldsymbol{\tau}}$. If $\mathrm{DR}_{\mathbf{x}} > \mathrm{DR}_{\boldsymbol{\tau}}$, then $\tau_k^\star < \mathrm{DR}_{\mathbf{x}} = x_k$. Therefore, to reconstruct the k-th entry of the input signal x_k, we always have a gap $\delta = x_k - \tau_k^\star > 0$ not covered by any sample to capture the amplitude information of $\mathbf{x}$. As a result, the desired signal is not found inside the finite-volume space imposed by the set of inequalities (8).

Using unlimited sampling framework, we now design the time-varying threshold with the same dynamic range as the modulo samples $\tilde{\mathbf{x}} = [\tilde{x}_k]$; i.e. $\mathrm{DR}_{\boldsymbol{\tau}} = \lambda$. We modify the thresholds to be closer to the clipping value thereby integrating self-reset ADC with one-bit sampling. The UNO sampling framework is summarized as follows:

1) Apply the modulo operator defined in (9) to the input signal $\mathbf{x}$ and obtain modulo samples $\tilde{\mathbf{x}} = \mathcal{M}_\lambda(\mathbf{x})$.
2) Design sequences of the time-varying sampling threshold $\left\{\boldsymbol{\tau}^{(\ell)}\right\}_{\ell=1}^{m}$ such that $|\mathrm{DR}_{\boldsymbol{\tau}^{(\ell)}} - \lambda| \leq \varepsilon_0$ for all $\ell \in \mathcal{L} = \{1, \cdots, m\}$ and a small number $\varepsilon_0 > 0$.
3) Apply the one-bit quantization to modulo samples as $\mathbf{r}^{(\ell)} = \mathrm{sgn}\left(\tilde{\mathbf{x}} - \boldsymbol{\tau}^{(\ell)}\right)$.

In order to derive a guarantee for the UNO threshold, we introduce a useful lemma as follows.

Lemma 1. *Assume $\boldsymbol{\tau}^{(\ell)} \sim \mathcal{N}\left(\mathbf{0}, \sigma_{\boldsymbol{\tau}}^2 \mathbf{I}\right)$. Then, with probability at least $1-\eta$, we have*

$$\left\|\boldsymbol{\tau}^{(\ell)}\right\|_\infty \leq \sigma_{\boldsymbol{\tau}} \sqrt{2\ln\left(\frac{2n}{\eta}\right)}. \tag{14}$$

Proof: According to the Hoeffding inequality and union bound for the Gaussian random variables $\boldsymbol{\tau}^{(\ell)} \sim \mathcal{N}\left(\mathbf{0}, \sigma_{\boldsymbol{\tau}}^2 \mathbf{I}\right)$, we have [32]

$$\Pr\left(\left\|\boldsymbol{\tau}^{(\ell)}\right\|_\infty \geq t\right) \leq 2n\, e^{-\frac{t^2}{2\sigma_{\boldsymbol{\tau}}^2}}. \tag{15}$$

Therefore, with $2n\, e^{-\frac{t^2}{2\sigma_{\boldsymbol{\tau}}^2}} \leq \eta$ proving the lemma. ∎

The following Proposition 1 states the UNO threshold design.

Proposition 1 (Judicious threshold design)**.** *Under the UNO sampling framework, the following* dynamic range guarantees *hold:*

- ***Gaussian threshold:*** *When $\boldsymbol{\tau}_{\mathcal{N}}^{(\ell)} \sim \mathcal{N}\left(\mathbf{0}, \sigma_{\boldsymbol{\tau}}^2 \mathbf{I}\right)$, then considering the ADC threshold λ, $\sigma_{\boldsymbol{\tau}}$ will be equal to $\frac{\lambda}{\sqrt{2\ln\left(\frac{2n}{\eta}\right)}}$ with a probability of at least $1-\eta$.*
- ***Uniform threshold:*** *When $\boldsymbol{\tau}_{\mathcal{U}}^{(\ell)} \sim \mathcal{U}_{[-a,a]}$, then $\lambda = a$ with a probability of 1.*

Proof: With a probability of at least $1-\eta$, the maximum amplitude of each threshold sequence is obtained via Lemma 1. When $\sigma_{\boldsymbol{\tau}} = \frac{\lambda}{\sqrt{2\ln\left(\frac{2n}{\eta}\right)}}$, then time-varying sampling threshold also has a DR of λ with a probability of at least $1-\eta$. The proof for the uniform threshold follows *mutatis mutandis* except that, for each ℓ, we have $\mathrm{DR}_{\boldsymbol{\tau}_{\mathcal{U}}^{(\ell)}} \leq a$ with a probability of 1 leading to $a = \lambda$. ∎

In Proposition 1, we design time-varying sampling threshold sequences so that their dynamic range is close to that of the modulo samples. This enables storing the information on the distance between the modulo samples and the thresholds without any loss of information via one-bit sampling.

V. RKA-Based Reconstruction

To reconstruct the signal of interest $\mathbf{x}^\star$ after UNO sampling, we rewrite the polyhedron (8) for modulo samples $\tilde{\mathbf{x}}$ as

$$\tilde{\mathcal{P}} = \left\{\tilde{\mathbf{x}} \mid \tilde{\boldsymbol{\Omega}}\tilde{\mathbf{x}} \succeq \mathrm{vec}\left(\mathbf{R}\right) \odot \mathrm{vec}\left(\boldsymbol{\Gamma}\right)\right\}. \tag{16}$$

To obtain the unlimited samples $\tilde{\mathbf{x}}$ in the polyhedron (16), it is required to solve a linear system of inequalities. We tackle this polyhedron search problem through RKA because of its optimal randomized projection and linear convergence in expectation [30]. The RKA is a *subconjugate gradient method* to solve overdetermined linear systems, i.e., $\mathbf{C}\mathbf{x} \preceq \mathbf{b}$, where $\mathbf{C}$ is a $m' \times n'$ matrix, $m' > n'$ [29, 30]. The conjugate-gradient methods immediately turn such an inequality to an equality of the following form:

$$\left(\mathbf{C}\mathbf{x} - \mathbf{b}\right)^+ = 0, \tag{17}$$

and then approach the solution by the same process as used for systems of equations.

Given a sample index set $\mathcal{J}$, without loss of generality, rewrite (17) as the polyhedron

$$\begin{cases} \mathbf{c}_j\mathbf{x} \leq b_j & \left(j \in \mathcal{I}_{\leq}\right), \\ \mathbf{c}_j\mathbf{x} = b_j & \left(j \in \mathcal{I}_{=}\right), \end{cases} \tag{18}$$

where the disjoint index sets $\mathcal{I}_{\leq}$ and $\mathcal{I}_{=}$ partition $\mathcal{J}$ and $\{\mathbf{c}_j\}$ are the rows of $\mathbf{C}$. The projection coefficient β_i of the RKA is [30, 33, 34]

$$\beta_i = \begin{cases} \left(\mathbf{c}_j\mathbf{x}_i - b_j\right)^+ & \left(j \in \mathcal{I}_{\leq}\right), \\ \mathbf{c}_j\mathbf{x}_i - b_j & \left(j \in \mathcal{I}_{=}\right). \end{cases} \tag{19}$$

The unknown column vector $\mathbf{x}$ is iteratively updated as

$$\mathbf{x}_{i+1} = \mathbf{x}_i - \frac{\beta_i}{\|\mathbf{c}_j\|_2^2}\mathbf{c}_j^{\mathrm{H}}, \tag{20}$$

where, at each iteration i, the index j is drawn from the set $\mathcal{J}$ independently at random following the distribution

$$\mathbb{P}\{j = k\} = \frac{\|\mathbf{c}_k\|_2^2}{\|\mathbf{C}\|_{\mathrm{F}}^2}. \tag{21}$$

Note that in (16), we have only the inequality partition $I_{\leq}$. Herein, $m' = m \times n$ and $n' = n$, and further, the row vector $\mathbf{c}_j$ and the scalar b_j used in the RKA (18)-(21) are j-th row of $-\tilde{\boldsymbol{\Omega}}$ and j-th element of $-\left(\mathrm{vec}\left(\mathbf{R}\right) \odot \mathrm{vec}\left(\boldsymbol{\Gamma}\right)\right)$, respectively. After reconstructing

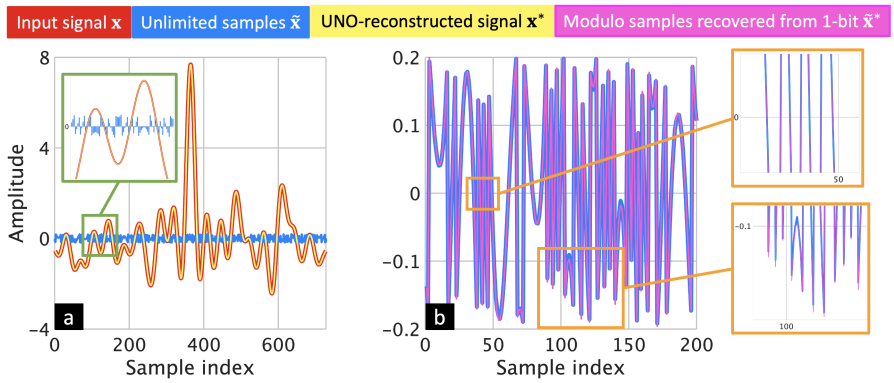

Figure 1. Illustration of UNO reconstruction when the ADC threshold $\lambda = 0.2$. (a) True signal $\mathbf{x}$, unlimited samples $\tilde{\mathbf{x}}$, and the reconstructed signal $\mathbf{x}^*$ obtained via RKA. (b) Modulo samples $\tilde{\mathbf{x}}$ and RKA-reconstructed modulo samples $\tilde{\mathbf{x}}^\star$ from one-bit measurements. The inset figures show the plots on a larger scale.

the modulo samples, the desired signal $\mathbf{x}$ is obtained from the approximated modulo samples using the unlimited sampling reconstruction procedure explained earlier in Section III.

VI. Numerical Illustrations

We assessed the performance of our UNO framework through numerical experiments. We set the ADC threshold to $\lambda = 0.2$. A total of 15 realizations of a bandlimited function x with piecewise constant Fourier spectrum were generated such that $\hat{x}(\omega) \in \mathcal{U}_{[0,1]}$. The number of time-varying sampling threshold sequences were set to $m = 400$. Throughout the experiments, the generated signals had the same dynamic range. Accordingly, we generated sequences of the time-varying sampling threshold as $\left\{\boldsymbol{\tau}^{(\ell)} \sim \mathcal{N}\left(\mathbf{0}, \frac{\lambda^2}{9}\mathbf{I}\right)\right\}_{\ell=1}^{m}$. We assess the reconstruction performance via the normalized mean square error (NMSE) defined as $\text{NMSE} \triangleq \frac{\|\mathbf{x}^\star - \bar{\mathbf{x}}\|_2^2}{\|\mathbf{x}^\star\|_2^2}$, where $\mathbf{x}^\star$ and $\bar{\mathbf{x}}$ denote the true discretized and the corresponding reconstructed signals, respectively.

Fig. 1a illustrates the RKA-based reconstruction performance of the UNO algorithm. UNO guarantees excellent reconstruction with the NMSE, averaged over 15 experiments, of the order $1e{-}6$. Fig. 1b shows the performance of RKA in unlimited samples reconstruction, which is at the heart of UNO framework, for the same signal as in Fig. 1a.

We compared the reconstruction performance of UNO with one-bit unlimited $\Sigma\Delta$ sampling of [27] for the same input signal. The ADC threshold was set to $\lambda = 1$ and sequences of the time-varying sampling threshold were generated following the procedure as before. Table I lists the reconstruction NMSE (on a $\log_{10}$ scale) for both sampling methods for different amplitudes $\|\mathbf{x}\|_\infty$. The UNO outperforms one-bit $\Sigma\Delta$ when the peak-signal-to-range (PSR) ratio $\eta = \frac{\|\mathbf{x}\|_\infty}{\lambda}$ becomes large, e.g., when $\|\mathbf{x}\|_\infty = 50$ for a fixed $\lambda = 1$. The degradation in one-bit $\Sigma\Delta$ reconstruction for large η is because of round-off noise in software and, primarily, imperfect noise shaping in sigma-delta conversion that results in sample corruption.

Fig. 2 compares the reconstruction using the Gaussian and uniform thresholds. Reconstruction with uniform thresholds exhibits lower errors than the Gaussian case because the former exploits the bit diversity after UNO sampling arising from the fact that the dynamic range of the generated time-varying thresholds is the same as the ADC threshold λ under UNO sampling architecture.

Table I
Reconstruction $\log_{10}$ NMSE for $\lambda = 1$

$\|\mathbf{x}\|_\infty$	One-bit unlimited $\Sigma\Delta$	UNO
20	0.0402	−6.3969
50	0.3777	−6.2081

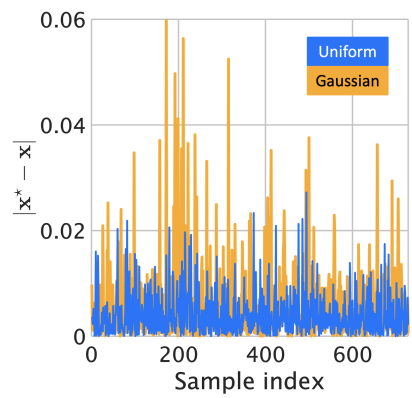

Figure 2. Element-wise absolute error in input signal reconstruction using Gaussian and uniform thresholds. The input signal is as in Fig. 1 with the amplitude $\|\mathbf{x}\|_\infty = 20$. Further, $\lambda = 1$ and $m = 400$. We generated Gaussian and uniform time-varying thresholds as $\left\{\boldsymbol{\tau}^{(\ell)} \sim \mathcal{N}\left(\mathbf{0}, \frac{1}{9}\mathbf{I}\right)\right\}_{\ell=1}^{m}$ and $\left\{\boldsymbol{\tau}^{(\ell)} \sim \mathcal{U}_{[-1,1]}\right\}_{\ell=1}^{m}$, respectively.

VII. Summary

We jointly addressed the problems of clipped inputs and high ADC power consumption through a new sampling framework, UNO, which naturally facilitates a judicious design of time-varying one-bit sampling thresholds. This method effectively utilizes the distance between the signal values and the thresholds in the wide dynamic range scenarios. Numerical examples show UNO signal reconstruction via RKA has very low NMSE. Numerical comparisons of reconstruction error between UNO and one-bit unlimited $\Sigma\Delta$ techniques show that the former is more robust in large PSR ratio scenarios.

Acknowledgement

The authors are grateful to Prof. Ayush Bhandari of Imperial College London for helpful discussions related to his work in [27], as well as for providing the relevant source codes for comparison.

REFERENCES

[1] C. E. Shannon, "Communication in the presence of noise," *Proceedings of the IRE*, vol. 37, no. 1, pp. 10–21, 1949.

[2] A. J. Jerri, "The Shannon sampling theorem – Its various extensions and applications: A tutorial review," *Proceedings of the IEEE*, vol. 65, no. 11, pp. 1565–1596, 1977.

[3] J. A. Hogan and J. D. Lakey, *Duration and bandwidth limiting: Prolate functions, sampling, and applications*. Springer, 2012.

[4] T. Olofsson, "Deconvolution and model-based restoration of clipped ultrasonic signals," *IEEE Transactions on Instrumentation and Measurement*, vol. 54, no. 3, pp. 1235–1240, 2005.

[5] A. Adler, V. Emiya, M. G. Jafari, M. Elad, R. Gribonval, and M. Plumbley, "Audio inpainting," *IEEE Transactions on Audio, Speech, and Language Processing*, vol. 20, no. 3, pp. 922–932, 2011.

[6] J. S. Abel, "Restoring a clipped signal," in *IEEE International Conference On Acoustics, Speech, and Signal Processing*, 1991, pp. 1745–1748.

[7] S. Ting and A. H. Sayed, "Mitigation of clipping in sensors," in *IEEE International Conference on Acoustics, Speech and Signal Processing*, 2013, pp. 5934–5938.

[8] A. Bhandari, F. Krahmer, and R. Raskar, "On unlimited sampling and reconstruction," *IEEE Transactions on Signal Processing*, vol. 69, pp. 3827–3839, 2020.

[9] F. Esqueda, S. Bilbao, and V. Välimäki, "Aliasing reduction in clipped signals," *IEEE Transactions on Signal Processing*, vol. 64, no. 20, pp. 5255–5267, 2016.

[10] V. Gregers-Hansen, S. M. Brockett, and P. E. Cahill, "A stacked A-to-D converter for increased radar signal processor dynamic range," in *IEEE Radar Conference*, 2001, pp. 169–174.

[11] D. Prasanna, C. R. Murthy, and C. Sriram, "On the application of modulo-ADCs for compressed sensing," in *Asilomar Conference on Signals, Systems, and Computers*, 2021, pp. 852–856.

[12] A. Bhandari, F. Krahmer, and R. Raskar, "On unlimited sampling," in *IEEE International Conference on Sampling Theory and Applications*, 2017, pp. 31–35.

[13] S. Rudresh, A. Adiga, B. Shenoy, and C. Seelamantula, "Wavelet-based reconstruction for unlimited sampling," in *IEEE International Conference on Acoustics, Speech and Signal Processing*, 2018, pp. 4584–4588.

[14] A. Ameri, J. Li, and M. Soltanalian, "One-bit radar processing and estimation with time-varying sampling thresholds," in *IEEE Sensor Array and Multichannel Signal Processing Workshop*, 2018, pp. 208–212.

[15] D. K. W. Ho and B. D. Rao, "Antithetic dithered 1-bit massive MIMO architecture: Efficient channel estimation via parameter expansion and PML," *IEEE Transactions on Signal Processing*, vol. 67, no. 9, pp. 2291–2303, 2019.

[16] A. Eamaz, F. Yeganegi, and M. Soltanalian, "One-bit phase retrieval: More samples means less complexity?" *IEEE Transactions on Signal Processing*, vol. 70, pp. 4618–4632, 2022.

[17] L. Jacques, J. Laska, P. Boufounos, and R. Baraniuk, "Robust 1-bit compressive sensing via binary stable embeddings of sparse vectors," *IEEE Transactions on Information Theory*, vol. 59, no. 4, pp. 2082–2102, 2013.

[18] J. H. Van Vleck and D. Middleton, "The spectrum of clipped noise," *Proceedings of the IEEE*, vol. 54, no. 1, pp. 2–19, 1966.

[19] A. Eamaz, F. Yeganegi, and M. Soltanalian, "Modified arcsine law for one-bit sampled stationary signals with time-varying thresholds," in *IEEE International Conference on Acoustics, Speech and Signal Processing*, 2021, pp. 5459–5463.

[20] C. Qian and J. Li, "ADMM for harmonic retrieval from one-bit sampling with time-varying thresholds," in *IEEE International Conference on Acoustics, Speech and Signal Processing*, 2017, pp. 3699–3703.

[21] A. Eamaz, F. Yeganegi, and M. Soltanalian, "Covariance recovery for one-bit sampled non-stationary signals with time-varying sampling thresholds," *IEEE Transactions on Signal Processing*, vol. 70, pp. 5222–5236, 2022.

[22] ——, "Covariance recovery for one-bit sampled stationary signals with time-varying sampling thresholds," *Signal Processing*, vol. 206, p. 108899, 2023.

[23] V. K. Goyal, M. Vetterli, and N. T. Thao, "Quantized overcomplete expansions in IR^n: Analysis, synthesis, and algorithms," *IEEE Transactions on Information Theory*, vol. 44, no. 1, pp. 16–31, 1998.

[24] P. T. Boufounos, "Universal rate-efficient scalar quantization," *IEEE Transactions on Information Theory*, vol. 58, no. 3, pp. 1861–1872, 2011.

[25] J. N. Laska, P. T. Boufounos, M. A. Davenport, and R. G. Baraniuk, "Democracy in action: Quantization, saturation, and compressive sensing," *Applied and Computational Harmonic Analysis*, vol. 31, no. 3, pp. 429–443, 2011.

[26] J. N. Laska, P. Boufounos, and R. G. Baraniuk, "Finite range scalar quantization for compressive sensing," Rice University, Tech. Rep. ADA520202, 2009.

[27] O. Graf, A. Bhandari, and F. Krahmer, "One-bit unlimited sampling," in *IEEE International Conference on Acoustics, Speech and Signal Processing*, 2019, pp. 5102–5106.

[28] S. Khobahi and M. Soltanalian, "Signal recovery from 1-bit quantized noisy samples via adaptive thresholding," in *Asilomar Conference on Signals, Systems, and Computers*, 2018, pp. 1757–1761.

[29] T. Strohmer and R. Vershynin, "A randomized Kaczmarz algorithm with exponential convergence," *Journal of Fourier Analysis and Applications*, vol. 15, no. 2, pp. 262–278, 2009.

[30] D. Leventhal and A. S. Lewis, "Randomized methods for linear constraints: Convergence rates and conditioning," *Mathematics of Operations Research*, vol. 35, no. 3, pp. 641–654, 2010.

[31] S. Boyd, S. P. Boyd, and L. Vandenberghe, *Convex optimization*. Cambridge university press, 2004.

[32] R. Vershynin, *High-dimensional probability: An introduction with applications in data science*. Cambridge University Press, 2018, vol. 47.

[33] J. Briskman and D. Needell, "Block Kaczmarz method with inequalities," *Journal of Mathematical Imaging and Vision*, vol. 52, no. 3, pp. 385–396, 2015.

[34] L. Dai, M. Soltanalian, and K. Pelckmans, "On the randomized Kaczmarz algorithm," *IEEE Signal Processing Letters*, vol. 21, no. 3, pp. 330–333, 2013.